Molecular Crystals and Liquid Crystals Incorporating Nonlinear Optics
Publication details, including instructions for authors and subscription information:
http://www.tandfonline.com/loi/gmcl17

Ferromagnetism in Two-Dimensional Cr(II) Halide Salts: Neutron Scattering and Optical Experiments

Steven T. Bramwell [a], Bernard Briat [a b], Peter Day [a c], Peter J. Fyne [a], Michael T. Hutchings [a d], Francis Tasset [a c] & Jonathan R. G. Thorne [a]

[a] Inorganic Chemistry Laboratory, Oxford, 0X1 3QR, U.K.

[b] ESPCI Labo d'Optique Physique, 10 rue Vauquelin, Paris, 5, France

[c] Institut Laue-Langevin, 156X, 38042, Grenoble, France

[d] AERE Harwell, Didcot, Oxon, 0X11 ORA, U.K.

Version of record first published: 22 Sep 2006.

To cite this article: Steven T. Bramwell , Bernard Briat , Peter Day , Peter J. Fyne , Michael T. Hutchings , Francis Tasset & Jonathan R. G. Thorne (1989): Ferromagnetism in Two-Dimensional Cr(II) Halide Salts: Neutron Scattering and Optical Experiments, Molecular Crystals and Liquid Crystals Incorporating Nonlinear Optics, 176:1, 451-464

To link to this article: http://dx.doi.org/10.1080/00268948908037502

Mol. Cryst. Liq. Cryst., Vol. 176, pp. 451–464
Reprints available directly from the publisher
Photocopying permitted by license only

Printed in the United States of America

FERROMAGNETISM IN TWO-DIMENSIONAL Cr(II) HALIDE SALTS: NEUTRON SCATTERING AND OPTICAL EXPERIMENTS.

STEVEN T. BRAMWELL, BERNARD BRIAT*, PETER DAY**, PETER J. FYNE, MICHAEL T. HUTCHINGS+, FRANCIS TASSET** AND JONATHAN R. G. THORNE
Inorganic Chemistry Laboratory, Oxford OX1 3QR, U.K.
*ESPCI Labo d'Optique Physique, 10 rue Vauquelin, Paris 5, France
**Institut Laue-Langevin, 156X, 38042 Grenoble, France
+AERE Harwell, Didcot, Oxon OX11 ORA, U.K.

Abstract Salts with formulae $A_2CrX_{4-y}Y_y$, where A = K^+, Rb^+, Cs^+, RNH_3^+ (R = alkyl or aryl); X = Cl, Y = Br, have layer structures based on that of K_2NiF_4. Near neighbour exchange in the two-dimensionally infinite CrX_2 lattice is ferromagnetic because of 'orbital ordering' induced by a cooperative Jahn-Teller distortion of X around the high spin $3d^4$ Cr(II). Curie temperatures (3D ordering) vary from 35 - 60 K with A, X and Y, though the ratio of intra- to interplanar exchange constants is at least 10^3. Inter-layer exchange can be tuned by varying the distance between the layers or the axial halide ligands. For the prototype compound Rb_2CrCl_4, polarized neutron diffraction has given information on the orbital occupancies that give rise to the ferromagnetic exchange, and optical experiments at very low temperatures (0.3 K) show how the spin-forbidden ligand field transitions in the visible couple to spin-waves in the ferromagnetic lattice.

INTRODUCTION

The tetrachlorochromate(II) salts, $A^I_2CrCl_4$ where A^I is a Group I cation or RNH_3^+, are rare examples of ionic insulators which order as ferromagnets (T_c = 35-50 K) (see Ref. 1 for a review).[1] They are also unusual in having well defined aborption bands in the visible, whose intensity is strongly reduced with the onset of magnetic order. The crystal structure of the prototype compound Rb_2CrCl_4 is related to the tetragonal K_2NiF_4 structure but because the high spin $3d^4$ configuration of the Cr^{2+} has a ground state ^5E_g in octahedral ligand field, the corner-sharing $CrCl_6$ units are subject to a Jahn-Teller distortion. The latter takes the form of a tetragonal elongation with the principal axis lying within the basal plane. The site group of the Cr^{2+} is D_{2h}, for which the ground term becomes ^5A_g and the electron configuration of the Cr^{2+} is expected to be $(xz)^1(yx)^1(xy)^1(z^2)^1(x^2-y^2)^0$, where z is the local principal axis of

the elongation. This ground configuration has been verified by polarized neutron diffraction[2,3] and we give a brief account of this important technique as applied to Rb_2CrCl_4.

The actual Cr-Cl bond lengths in Rb_2CrCl_4 approximate quite closely to a D_{4h} ligand field and the ground term then becomes $^5B_{1g}(^5E_g\varepsilon)$. Alternate $CrCl_6$ are elongated along the [100] and [010] axes of the parent K_2NiF_4 cell, so that z-axes of neighbouring Cr^{2+} are orthogonal.[4,5,6] Superexchange between the half-filled z^2 orbital on one site and the empty x^2-y^2 on the next, via the $3p\sigma$ orbital of the bridging Cl^-, assures a ferromagnetic near neighbour exchange.[7] The ^5A_g ground term suffers a zero-field splitting because of second-order mixing with excited states due to spin-orbit coupling. This gives rise to a single ion anisotropy term D constraining the moments in the basal plane and a further term P which, in the absence of exchange, would constrain neighbouring moments alternately along [100] and [010]. The result of the competition between the ferromagnetic exchange and the orthogonal directions of P on neighbouring cations is a magnetic structure having the easy direction along [110] but with alternate moments canted a few degrees to either side of this axis.[6]

The unusual temperature dependence of the visible absorption bands in Rb_2CrCl_4 has been the subject of numerous studies.[8-10] Attention has concentrated on two regions near 630 and 530 nm. In both regions the integrated band intensity obeys a T^2 temperature dependence 4-50K. Since the bands are due to quintet-triplet ligand field transitions, their electric-dipole intensity is derived from coupling the creation of such an exciton with annihilation of a thermally populated magnon.[8] The intensity is therefore determined by the Bose population of the magnons. Closer inspection of the 631 nm absorption region between 0.8 and 4.2 K revealed a deviation from the T^2 intensity law expected for a square planar Heisenberg ferromagnet with small anisotropy, because in this temperature range the thermal energy becomes comparable to the anisotropy gap in the magnon dispersion at the Brillouin zone centre.[9] Furthermore, when the temperature is low enough to remove most of the intensity from the magnon annihilation sideband ('hot' band), a weak magnon creation sideband ('cold' band) becomes apparent. It is rendered allowed by the small antiferromagnetic component in the structure, which arises from the canting.

Application of a magnetic field along [110], [100] or [001] at a fixed temperature causes an overall reduction in the intensity of the

major bands at 631, 523, 534 and 532 nm because the magnon dispersion surface is shifted by the Zeeman energy and the magnon population is changed.[11] More subtle effects may be anticipated, however, because the zone-centre anisotropy gap is not a monotonic function of field applied along the hard [100] and [001] axes because the moments must rotate first into the direction of the field.[12] For example, the critical field needed to bring the moments from [110] to the [100] direction has been found by inelastic neutron scattering to be 0.21T.[13] It has also been observed that several bands, e.g. at 632 and 625 nm, shift with field much more than one would anticipate for a Zeeman splitting with g ~ 2. The same bands also increase in intensity very markedly with applied field.[11]

The present paper surveys optical and magneto-optical data for Rb_2CrCl_4 as a function of temperature and magnetic field applied along [110] and [100], and outlines a quantitative discussion of the band shapes and energy shifts. We describe absorption spectra for the 631 nm region down to 0.35 K in zero field, which enables us to locate the exciton origin line and hence the energies of the magnon creation and annihilation bands on each side of it.

POLARIZED NEUTRON DIFFRACTION

The electron configuration of Cr^{2+} is high spin $(3d)^4$. Qualitative crystal field arguments suggest that elongating the $CrCl_6$ octahedra splits the e_g subshell so that (z^2) is half filled and (x^2-y^2) empty, where z is the local coordinate of the elongation. 'Orbital ordering' of this kind provides the microscopic mechanism of the ferromagnetic exchange in the isostructural $3d^9$ compound K_2CuF_4,[14] and these arguments were extended to the $3d^4$ configuration[7] to determine to what extent such orbital ordering exists in Rb_2CrCl_4 by making a quantitative examination of the spatial distribution of unpaired spin density. Since superexchange between the half filled (z^2) on one Cr^{2+} and the empty (x^2-y^2) on its neighbours is likely to be the dominant mechanism for the exchange interaction, it is also of interest to estimate the fraction of unpaired spin transferred to the bridging Cl^- ions in the basal plane.

To model the observed magnetic structure factors (F_{Mobs}) we consider the magnetization density as a superposition of unpaired spin densities arising from the occupation of individual atomic orbitals on

each atom, which are represented by form factors which take account of the local site symmetry. Occupancy of each orbital is determined by least squares fitting to the F_{Mobs}.

The cross section for the interaction of polarized neutrons with a ferromagnetic sample is:[15]

$$\sigma^{P}(Q) = F_N^2(Q) + q^2F_M^2(Q) + 2q^2PF_N(Q)F_M(Q) \qquad (1)$$

where $F_N(Q)$ and $F_M(Q)$ are the nuclear and magnetic structure factors and q^2 equals $\sin^2\alpha$ where α is the angle between the scattered vector Q and the moment direction and P is the degree of the incident polarization. For perfectly polarized neutrons, $P = \pm 1$ so that for each Bragg reflection the 'flipping ratio' for a reversal of the direction of polarization is,

$$R(Q) = \frac{\sigma^{+}(Q)}{\sigma^{-}(Q)} = \frac{F_N^2(Q) + q^2F_M^2(Q) + 2q^2F_N(Q)F_M(Q)}{F_N^2(Q) + q^2F_M^2(Q) - 2q^2F_N(Q)F_M(Q)} \qquad (2)$$

For a symmetrical crystal such as Rb_2CrCl_4,

$$R(Q) = \frac{\gamma^2(Q) + 2\gamma(Q) + (1/q^2)}{\gamma^2(Q) - 2\gamma(Q) + (1/q^2)} \qquad (3)$$

where $\gamma(Q) = F_M(Q)/F_N(Q)$ is the ratio of two real quantities. $\gamma(Q)$ is determined from the experiment, and if $F_N(Q)$ is already known from an unpolarized neutron diffraction experiment, $F_M(Q)$ can be found.

The crystal was cooled in a 5T cryomagnet to 4.5 K. Data were collected on the D3 polarized neutron diffractometer at the Institut Laue-Langevin, Grenoble. The flipping ratios of 660 main structure reflections (189 independent reflections) were measured up to $\sin\theta/\lambda \leq 0.8$ Å^{-1}. To model F_{Mobs} we followed Schweizer and Tasset[16] and considered the magnetization density as a superposition of independent densities from individual electrons with unpaired spin in specified orbitals centered at the magnetic ions. The calculated structure factor is given by

$$F_{Mcalc}(Q) = \sum_j \sum_k \sum_p m_{j,k} f_p^{j,k}(Q) \exp(iQ \cdot r_{j,k}) \exp(-W_j), \qquad (4)$$

where $m_{j,k}$ is the moment, $f_p^{j,k}$ is the magnetic form factor of an electron in orbit p on atom of type j, and $r_{j,k}$ is the position of the jth type atom at the kth position in the unit cell. The orbital form factor of a 3d electron is assumed to be isotropic[15] and equal to

$$f_i(Q) = \langle j_o(Q)\rangle + \langle j_2(Q)\rangle, \tag{5}$$

where the radial integrals $\langle j_o\rangle$, $\langle j_2\rangle$ are related to the mono-electronic wavefunction. Thus the overall structure factor for Cr(3d) is given by a summation of contributions from each orbital weighted by its fractional occupancy n(orb):

$$F_{Mcalc}Cr(3d) = \gamma m[Cr(3d)] \sum_{jk} \{\nu[n(3d_{z^2})f[j,3d_{z^2}] + n(3d_{xz})f[j,3d_{xz}]$$

$$+ n(3d_{yz})f[j,3d_{yz}] + n(3d_{x^2-y^2})f[j,3d_{x^2-y^2}] + n(3d_{xy})f[j,3d_{xy}]]$$

$$+ (1-\nu)[\langle j_o(Q)\rangle + \langle j_2(Q)\rangle]\} \exp(iQ\cdot r_{j,k})\exp(-W_{Cr}), \tag{6}$$

where $\gamma = 0.2695[10^{-12}$ cm $\mu_B]$ and m[Cr(3d)] is the localized magnetic moment on one Cr atom in Bohr magnetons (μ_B), and ν and $(1-\nu)$ are respectively the spin and orbital proportions for the spin and orbital form factor respectively. Note that $n(3d_{z^2}) = n(3d_{xz}) = n(3d_{yx}) = n(3d_{x^2-y^2}) = n(3d_{xy}) = 0.2$ represents a spherical distribution of the moment density. Any deviation from these values signifies an aspherical distribution.

The main conclusion from fitting different atomic models to the observed magnetic structure factors of Rb_2CrCl_4 is a strong vindication of the concept of 'orbital ordering' in compounds with cooperative Jahn-Teller distortions. The results are listed in Table I.

Even the crudest model, which assumes that the spin density is confined to the Cr(3d) orbitals (fit 1, table I), shows quite clearly that the moment is distributed almost equally between xz, yz, xy and z^2 orbitals, with x^2-y^2 unoccupied. Though the distribution of the moment between the four occupied orbitals is not required to be equal by symmetry, in no case does the proportion of the total 3d moment occuping any of these orbitals deviate from 25% by an amount greater than the standard deviation. The refinements indicate the proportion of the moment arising from orbital angular momentum to be zero, though the crude Cr(3d) model fails to account for the whole moment since

TABLE I Parameters from least squares fit of F_{Mcalc} to the F_{Mobs} from polarized neutron diffraction experiment on Rb_2CrCl_4 (Ref. 3).

Refined parameters	Fit Number 1	2	3
m[Cr(3d)][μ_B]	3.51(3)	3.50(4)	3.16(8)
ν(Cr(3d))	1.08(2)	1.07(2)	0.97(3)
n($Cr3d_z2$)	0.26(2)	0.26(2)	0.25(2)
n($Cr3d_{x^2-y^2}$)	-0.02(2)	-0.03(2)	-0.01(2)
n($Cr3d_{yz}$)	0.24(1)	0.24(1)	0.26(2)
n($Cr3d_{xz}$)	0.24(1)	0.23(1)	0.25(2)
n($Cr3d_{xy}$)	0.29(—)	0.29(—)	0.25(—)
m[Cl(1)3p][μ_B]	-	0.08(3)	0.06(3)
n($Cl(1)3p_x$)	-	0.6(3)	0.9(1)
n($Cl(1)3p_y$)	-	0.8(3)	0.7(4)
m[Cl(2)3p][μ_B]	-	0.08(5)	0.08(5)
n($Cl(2)3p_x$)	-	0.4(3)	0.5(2)
n($Cl(2)3p_y$)	-	0.2(3)	0.3(3)
m[Cl(1)3s][μ_B]	-	-	-
m[Cl(2)3s][μ_B]	-	-	-
m[Cr(1)4s][μ_B]	-	-	0.6(1)
R′	0.00882	0.00839	0.00767

$R' = [\Sigma(F_{Mobs} - F_{Mcalc})^2/\delta F^2_{Mobs}]/[\Sigma F^2_{Mobs}/\delta F^2_{Mobs}]$;
$1/\delta F_{Mobs}$ is the weight attached to each F_{Mobs} where δF_{Mobs} is its standard deviation.

the refined value of $3.51(3)\mu_B$ falls appreciably below the expected $4\mu_B$. Including Cr(4s) and Cl(3s,3p) improves the situation appreciably, giving the total moment of $3.86\mu_B$.

Since the distance between nearest neighbour Cr^{2+} in Rb_2CrCl_4 is 5.09 Å, it can be assumed that direct exchange between 3d orbitals does not play a significant role in the magnetic ordering mechanism and that cation-anion-cation superexchange[17] is the dominant process. The topology of the cation and anion array within the basal plane is such that only 180° superexchange need be considered.

With the 3d orbital populations experimentally determined, the 'orbital ordering' mechanism for the ferromagnetic exchange in

K_2CuF_4 [14] can be extended to explain the ferromagnetism of Rb_2CrCl_4. Because of the cooperative Jahn-Teller distortion, the half-filled z^2 orbital on Cr1 overlaps with the $3p_z$ orbital on Cl(1), which in turn overlaps with the empty x^2-y^2 orbital on Cr2. The latter orbital is orthogonal to the half-filled z^2 on the same centre, so intra-atomic electron repulsion is minimized when the transferred spin in x^2-y^2 is parallel to that in the z^2 orbital, and likewise to the spins in the other three half-filled 3d orbitals. This conclusion agrees with the arguments of Eremin & Kalinenkov[7].

Central to the superexchange mechanism is a degree of cation-anion covalency. There is no real difference in the proportions of the Cl(3p) moment occupying x or y orbitals on either site, though there is some indication that spin declocalization is greater through the p_σ than the p_π orbitals. This agrees with polarized neutron diffraction data on the discrete $CoCl_4^{2-}$ complex in Cs_3CoCl_5. However, the magnitude of the total 3p moment shared between Cl(1) and Cl(2) in Rb_2CrCl_4 (0.14 μ_B) is distinctly greater than the Cl(3p) moment in $CoCl_4^{2-}$(0.08 μ_B).

SPIN WAVES IN A MAGNETIC FIELD

To understand the optical absorption spectrum and the effect on it of temperature and magnetic fields, we need to examine the magnetic excitations (spin waves) in a two-dimensional square easy-plane ferromagnet. This problem has been treated in several papers[11,12,18] so we shall briefly summarize the conclusions. Since alternate $CrCl_6$ octahedra (i and j) in the layers of the tetrahalogenochromates(II) are elongated along [100] and [010] of the K_2NiF_4 unit cell, we use a two-sublattice model. With the notation of Fig.1, the spin Hamiltonian in the absence of a magnetic field is[12]

$$\mathcal{H} = -\sum_{i,j} J(S_{i1}\cdot S_{j2}) - P\{\sum_i S^2_{iz_1} + \sum_j S^2_{jz_2}\} + D\{\sum_i S^2_{iy_1} + \sum_j S^2_{jy_2}\} \qquad (7)$$

where J stands for the nearest-neighbour exchange interaction between spins in the (001) plane. The easy axis of magnetization is [110] but, due to the P terms, the spins on the two sublattices i, j are canted at a small angle to this direction.

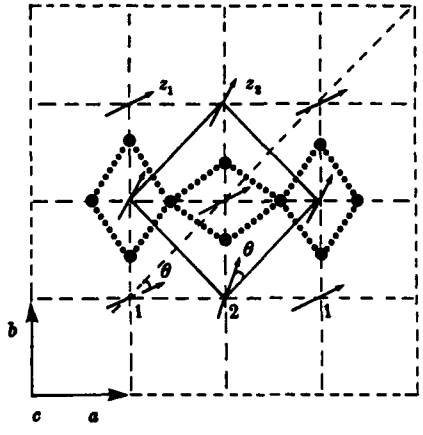

FIGURE 1. Magnetic and crystal structures of Rb_2CrCl_4 in the (001) plane. Canted spins lie along z_1 and z_2 in sublattices 1 and 2 respectively with the angle θ exaggerated.

At T=0 the diagonalized spin-wave Hamiltonian has an acoustic (E_+) and an optic (E_-) branch with energies which vary with wavevector k as follows:

$$(E\pm)^2 = \{4SJ\ (\cos 2\theta \mp \gamma) + S[2D + P\ (1 + \sin 2\theta)]\}\ \{4SJ \cos 2\theta\ (1 \mp \gamma) + 2SP \sin 2\theta\} \quad (8)$$

where $\gamma = (1/4) \sum_{Ri} \exp(ik.R_i)$. The two branches meet at the zone boundary where $\gamma = 0$ and $E \simeq 4SJ$ since the P and D terms are small relative to the J term. The canting angle θ is given by $\tan 2\theta = P/4J$. At the zone centre, $E_- \simeq 8SJ$ and a small gap also appears in the acoustic branch:

$$(E0)^2 \simeq P^2S^2\ (P + 2D)/2J \quad (9)$$

Next it is worth summarizing the effect of a magnetic field on the spin waves.[12] Let $E_Z = g\mu_B.H$ be the Zeeman energy. With the field along the energy [110] axis, the gap energy varies as:

$$(E_+)^2 \simeq (E0)^2 + (E_Z)^2 + E_ZS[2D + P] \quad (10)$$

while E_- varies linearly with E_Z at all fields. When a small field is applied in the [100] direction, the spins first rotate their mean

direction (fig. 1), making an angle ϕ with [100]. One finds $E_z = (P^2/J)\cos\phi \cos 2\phi$. At the same time Θ decreases according to the law $\Theta = (P/8J) \sin 2\phi$ so that the gap becomes zero for $E_z = (P^2/J)$. This gives the field required to pull the canted spins into the [100] direction. At sufficiently high fields (1.5 T), E_+ follows Eq.(10) approximately.

Finally, when H is parallel to [001], the mean field direction makes an angle ϕ with [110] and one finds approximately:

$$E_z = \sin\phi \, [P^2 + 8J \, (P + 2D)/4J$$
$$\Theta = \cos\phi \, [(E_z/PS \sin\phi) - (2 + D/P)] \qquad (11)$$

It can be seen that both the gap energy and Θ go to zero for $E_z \sim 2(P + 2D)$ while for higher fields, E_+ increases monotypically with a slope given by Eq.(10).

The parameters given in ref. 19 ($J = 10.6$ cm^{-1}, $P = 1.65$ cm^{-1} and $D = -0.22$ cm^{-1}) lead to $E0 = 0.79$ cm^{-1} and a canting angle in zero external field of 1.1°. Assuming a g factor of 2, the critical magnetic fields H_c for turning the spins towards [100] anbd [001] are therefore 0.276 T and 2.67 T respectively. The magnetic field dependence of the zone centre gap energy calculated from these parameters is shown in Fig.2(a). In fact, this variation has been measured at 4.2 K by long wavelength (6Å) inelastic neutron scattering for H // [100] using the IN12 spectrometer at the Institut Laue-Langevin, Grenoble, with the results shown in Fig. 2(b).[13]

OPTICAL ABSORPTION SPECTRUM: MAGNON CREATION AND ANNIHILATION SIDEBANDS

It is found experimentally that cooling the crystal to very low temperature eliminates the annihilation band while the intensity of the creation band remains constant below 1K and decreases only slowly above that temperature[6,10] (Fig. 3(a)). Applying a field along [100] > H_c makes both sidebands less intense, with the creation band moving away from the annihilation one, the latter remaining almost unchanged in energy (Fig. 4(a)). This arises from the fact that, when the magnon energy is a linear function of field, the increasing energy gained from destroying a magnon offsets the increasing energy needed to create an exciton. The creation sideband shows a larger shift

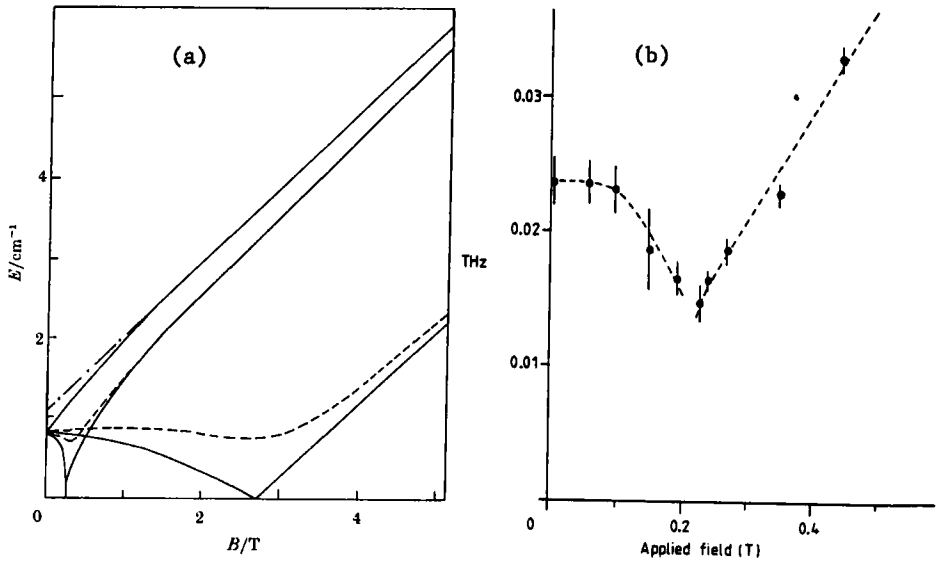

FIGURE 2. (a) Calculated field dependence of the acoustic gap for H along [110] (upper curves), [100] (intermediate) and [001] (lower curves) respectively. The dotted lines reflect a 5° misalignment of the field off the above axes in the (001) or the (1$\bar{1}$0) plane (g = 2, J = 10.4 cm^{-1}, P = 1.65 cm^{-1} and D = -0.22 cm^{-1}). (b) Measured field dependence of the acoustic gap for H along [100].[13]

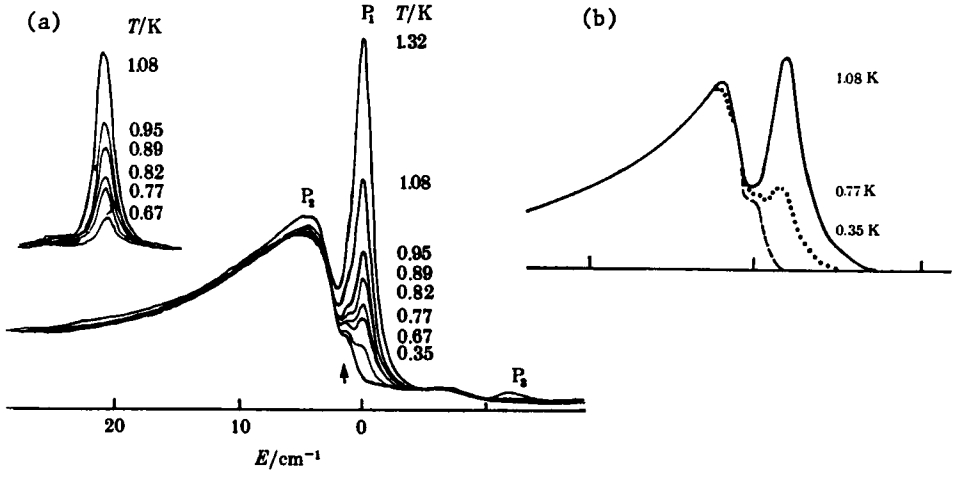

FIGURE 3. Absorption spectra for region I of Rb_2CrCl_4 at very low temperatures. (a) Observed spectra. The inset shows the temperature-dependence of the hot band. (b) Simulations (J,P,D,g parameters listed in text).

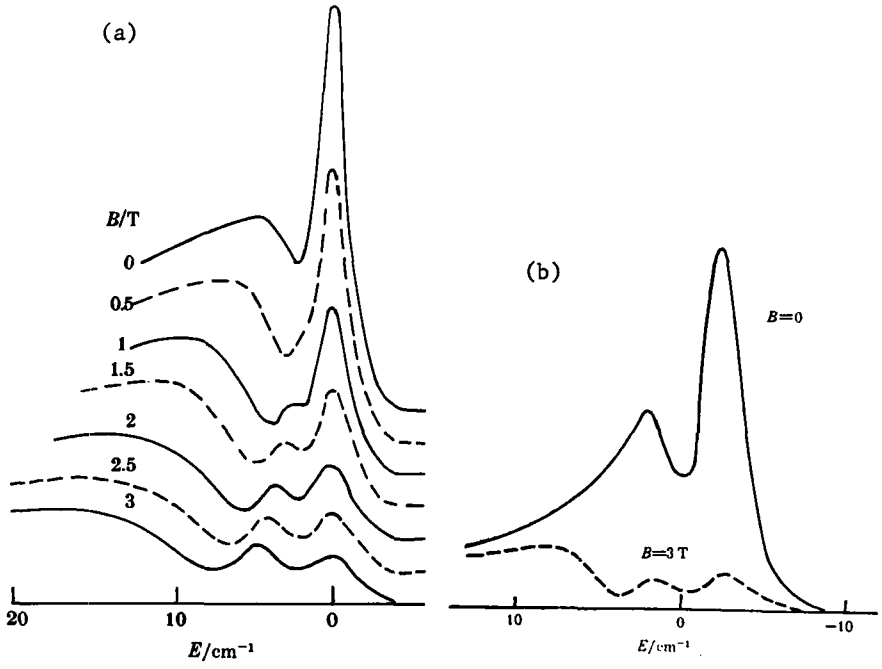

FIGURE 4. Influence of a magnetic field H // [100] in region I at 1.4 K. (a) Observed spectra, (b) Simulations (J,P,D,g parameters listed in text).

because the extra energy required to create the magnon adds to that of the exciton. The band shapes for the magnon annihilation (hot) and creation (cold) sidebands have been calculated rigorously in the absence or presence of a 'large' external magnetic field ($H \gg H_c$) by numerical methods, taking account of all the points in the Brillouin zone.[10,12,18]

To follow the intensity and shift of the hot band in a small magnetic field, one can use a simplified model, which we shall describe briefly. For details of the full calculations, see ref. 10. Quite generally, the absorbance can be written (apart from a constant multiplicative factor) as

$$A = |M|^2 n \rho \tag{12}$$

where M is the effective dipole movement associated with the transition; n is given by the Bose-Einstein law

$$n = [\exp(E/kT - 1)]^{-1} \tag{13}$$

E is the magnon energy and ρ is the magnon density of states at energy E. In the limit where $k \sim 0$, E is given by

$$E = E(0) + \alpha k^2 \tag{14}$$

Moreover, M varies as $(\sin^2 k_x R + \sin^2 k_y R)$, i.e. as k^2 at low k. For a two-dimensional Bravais lattice, one has

$$\rho = \frac{1}{2\pi} k \frac{dk}{dE} = \text{constant at low k} \tag{15}$$

Finally, the profile of the hot band is calculated using the relationship $A = (E-E(0))\ [\exp(x) - 1]^{-1}$ where $x = E/kT$. When a magnetic field is applied, we substitute E(G) for E(0), E(G) being given by eq.(10) ($E(G) \equiv E_+$) for H // [110] or fig. 2(a) for the field in the two other directions.

The calculated temperature and field dependence of the sidebands is shown in figure 5(b) for H approximately along [100]. As expected from the spin-wave behaviour, the hot band now undergoes a slight blue shift when H increases from 0 up to the critical field H_c with a

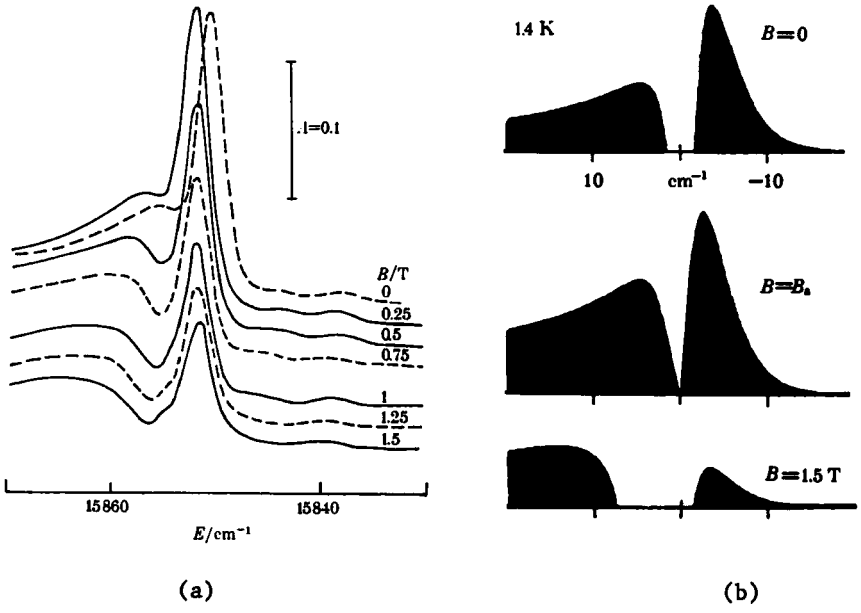

FIGURE 5. Influence of a magnetic field B//[100] in region I at 1.8K. (a) Observed spectra, (b) Simulations (at 1.4K; J,D,P,g parameters listed in text).[10]

simultaneous increase of the intensity. For H lying between H_c and about 1T, a small shift of the maximum is seen in the opposite direction because the gap is now increasing again (figure 2(a)). Above 1T the position of the hot band is field-independent because the increasing energy of the gap is compensated by the increased energy of the exciton. Again, these findings are in very good qualitative agreement with experimental data.[10]

A difference between the experiments and theory is that, experimentally, the gap between the hot and cold bands, e.g. in Fig. 5, is partially filled. This is because the width of the exciton absorption line (0.9 cm^{-1}) is not insignificant compared to the width of the sideband. A similar gaussian distribution should therefore be given to each k-point in the lineshape function. Then the hot band has a symmetrical profile (Fig. 3(b)), as found experimentally, and the exciton appears as a shoulder between the two bands. The most interesting observation, however, is that the ratio of the hot-band : cold-band intensities depends very critically upon the relative values of the two parameters P and D. Thus the simulation demonstrates conclusively that D is negative, as can be verified by comparing the theoretical results in figures 3(b) and 4(b) with the experimental data in figures 3(a) and 4(a). Excellent fits are obtained by using the following set of parameters: $J = 10.42\ cm^{-1}$, $P = 1.55\ cm^{-1}$ and $D = -0.22\ cm^{-1}$. These lead to $H_a = 0.25$ T, $H_c = 2.54$ T, $E_a = 0.75\ cm^{-1}$ and $E_o = 168.0\ cm^{-1}$, in quite satisfactory agreement with all the optical, magnetic resonance and neutron scattering experiments.

CONCLUSIONS

The optical and magnetic behaviours of the prototype ionic ferromagnet Rb_2CrCl_4 are now very well understood, both qualitatively and quantitatively. The reason why it is ferromagnetic has been established from the 'orbital ordering' determined by polarised neutron diffraction. The variation of the magnetic excitations (spin waves or magnons) with wavevector and applied field has been measured and related to the equilibrium canted spin structure. Knowledge of the spin waves leads to detailed simulation of the lineshapes of the visible absorption bands and the way in which they change with temperature and applied field. It remains to apply the recipe to construct other ferromagnetic lattices with unusual optical properties.

ACKNOWLEDGEMENTS

Over the years, our work on tetrahalogenochromates(II) has been supported by many agencies: SERC, AERE Harwell, CNRS, ILL Grenoble, the Royal Society and the British Council.

REFERENCES

1. P. Day, Acc. Chem. Res., 12, 236 (1979).
2. G. Münninghoff, E. Hellner, P. J. Fyne, P. Day, M. T. Hutchings and F. Tasset, J. Physique, Colloq., C7, 243 (1982).
3. P. Day, P. J. Fyne, E. Hellner, M. T. Hutchings, G. Münninghoff and F. Tasset, Proc. Roy. Soc., A406, 39 (1986).
4. P. Day, E. Janke, T. E. Wood and D. Woodwark, J. Phys. C. Sol. St. Phys., 12, L279 (1979).
5. G. Münninghoff, W. Treutmann, E. Hellner, G. Heger and D. Reiner, J. Sol. St. Chem., 34, 289 (1980).
6. E. Janke, M. T. Hutchings, P. Day and P. J. Walker, J. Phys. C. Sol. St. Phys., 16, 5959 (1983).
7. M. V. Eremin and V. N. Kalinenikov, Sov. Phys. Sol. St., 20, 205 (1978).
8. A. K. Gregson, P. Day, A. Okiji and R. J. Elliott, J. Phys. C. Sol. St. Phys., 9, 4497 (1976).
9. P. Day, M. T. Hutchings, E. Janke and P. J. Walker, J. Chem. Soc., Chem. Commun., 711 (1979).
10. B. Briat, S. T. Bramwell, J.C. Canit, P. Day and J. R. G. Thorne, Proc. Roy. Soc., A415, 277 (1988).
11. E. Janke, T. E. Wood, C. N. Ironside and P. Day, J. Phys. C. Sol. St. Phys., 15, 3809 (1982).
12. M. C. Harrop, D. Phil. Thesis, Oxford University (1981).
13. P. J. Fyne, P. Day, M. T. Hutchings, S. Depinna, B. C. Cavennett and R. Lynn, J. Phys. C. Sol. St. Phys., 17, 1281 (1984).
14. D. I. Khomskii and K. I. Kugel, Solid St. Commun., 13, 763 (1973).
15. W. Marshall and S. W. Lovesey, The Theory of Thermal Neutron Scattering (Oxford University Press 1971).
16. J. Schweizer and F. Tasset, J. Phys. F., 10, 2799 (1980).
17. P. W. Anderson, Phys. Rev., 115, 2 (1959).
18. R. J. Elliott, A. Hengeltraub, M. C. Harrop and T. A. L. Ziman, J. Mag. Mag. Mat., 15-18, 359 (1980).
19. M. T. Hutchings, J. Als-Neilsen, P. A. Lindgard and P. J. Walker, J. Phys. C. Sol. St. Phys., 14, 5327 (1981).